Analysis of signal-dependent sensor noise on JPEG 2000-compressed Sentinel-2 multi-spectral images

M. Uss[a], B. Vozel[b], V. Lukin [a], K. Chehdi[b]
[a]Department of Transmitters, Receivers and Signal Processing, National Aerospace University, Kharkov, Ukraine; [b]IETR UMR CNRS 6164 - University of Rennes 1, CS 80518, 22305 Lannion cedex, France;

ABSTRACT

The processing chain of Sentinel-2 MultiSpectral Instrument (MSI) data involves filtering and compression stages that modify MSI sensor noise. As a result, noise in Sentinel-2 Level-1C data distributed to users becomes processed. We demonstrate that processed noise variance model is bivariate: noise variance depends on image intensity (caused by signal-dependency of photon counting detectors) and signal-to-noise ratio (SNR; caused by filtering/compression). To provide information on processed noise parameters, which is missing in Sentinel-2 metadata, we propose to use blind noise parameter estimation approach. Existing methods are restricted to univariate noise model. Therefore, we propose extension of existing vcNI+fBm blind noise parameter estimation method to multivariate noise model, mvcNI+fBm, and apply it to each band of Sentinel-2A data. Obtained results clearly demonstrate that noise variance is affected by filtering/compression for SNR less than about 15. Processed noise variance is reduced by a factor of 2 - 5 in homogeneous areas as compared to noise variance for high SNR values. Estimate of noise variance model parameters are provided for each Sentinel-2A band. Sentinel-2A MSI Level-1C noise models obtained in this paper could be useful for end users and researchers working in a variety of remote sensing applications.

Keywords: remote sensing, Sentinel-2, MultiSpectral Instrument, blind noise parameter estimation, multivariate noise variance model, signal-dependency, processed noise, image denoising, image compression.

1. INTRODUCTION

The Sentinel-2 satellites acquires multi-spectral images with 13 bands covering visible, near infrared and short wave infrared part of the spectrum [1]. The application range of these data includes but is not limited to risk management, land use, forest monitoring, water management, soil protection, urban mapping.

An important characteristic of a remote sensing sensor is its signal-to-noise ratio (SNR) influencing quality of products derived from the sensor data. SNR is related to the sensor noise parameters, knowledge of which is needed for performing data filtering, image segmentation, spectral unmixing, or classification. Sensor noise parameters are determined during pre-flight sensor calibration and later controlled during in-flight calibration process. However, freely distributed Sentinel-2 Level-1C data lack detailed information on the sensor noise properties.

Alternatively, sensor noise properties can be analyzed directly from the noisy data by blind noise parameter estimators [2]. For Sentinel-2, application of existing blind noise parameter estimators is problematic. First, Level-1C images undergo filtering and are distributed in JPEG2000 compressed form. Image filtering/compression modifies noise both in the sense of its statistics and spatial correlation width [3]. The strength of filtering effect is data-dependent [4], i.e., may locally vary over image area depending on such factors as local SNR, image texture roughness and anisotropy, presence of small-sized objects or edges [5, 6]. Apart from this, noise for optical sensors inherently depends on image intensity [2]. This makes noise model of compressed data multivariate, the kind of problem state-of-the-art noise parameter estimators cannot deal with. Second, noise parameter estimators of multichannel data work under assumption that all bands are represented at the same spatial grid [7]. This is not the case for Sentinel-2 image data: bands have different spatial resolution (10, 20, 60m) and non-negligible inter-band misregistration.

In the paper, we overcome the above mentioned difficulties by modifying previously proposed noise parameter estimator vcNI+fBm (Vector estimator of spatially Correlated noise using Noise Informative areas and Fractal Brownian Motion

[a] Correspondence to M. Uss: e-mail uss@xai.edu.ua tel./fax +380503013333

model) [8] to the case of multivariate noise variance model. The new estimator is called mvcNI+fBm ("m" for multivariate). To cope with different spatial resolutions of MSI bands and, especially, their inter-band misregistration we propose to preprocess Sentinel-2 data before applying mvcNI+fBm. For a reference band, the preprocessing includes selection of bands with the same or finer spatial resolution, band mutual registration, interpolation to the reference band grid, and point spread function adjustment. Application of mvcNI+fBm to thus pre-processed multichannel image provides individual noise variance and spatial correlation width estimates that are further analyzed as a bivariate function of image intensity and local SNR.

In the experimental part of the paper, we analyze noise parameters of six Sentinel-2A granules. Analysis reveals that influence of both image intensity and local SNR on noise variance is significant. For a fixed SNR, noise variance model agrees with mixture of additive and scaled Poisson noises. For low SNR, the noise variance decreases approximately by a factor of 2-5 as compared to high SNR due to filtering and JPEG2000 compression. We have also analyzed noise spatial correlation width and obtained it about 0.45 pixels (one sigma, Gaussian spatial correlation function shape).

The remainder of this paper is organized as follows. We recall the main characteristics of MSI sensor onboard Sentinel-2 satellites in the beginning of Section II. Then, bivariate model of MSI sensor Level-1C data noise is introduced and discussed. We discuss the drawbacks of existing blind noise parameters estimators in case of Sentinel-2 data and propose mvcNI+fBm estimator that is able to work with multivariate noise model. In section III, we apply mvcNI+fBm estimator to six Sentinel-2A granules, confirm significance of both intensity and SNR influence on noise variance. Noise parameters estimates for each band of MSI sensor are provided. In concluding Section IV we summarize our work and give few remarks on future work.

2. PARAMETERS ESTIMATION OF SENTINEL-2 MSI SENSOR NOISE AT LEVEL-1C

2.1 Sentinel-2 sensor and data processing overview

The Sentinel-2 mission is a part of Copernicus Earth observation program directed by the European Commission in partnership with the European Space Agency (ESA). Apart from Sentinel-2, it includes Sentinel-1 Synthetic Aperture Radar (SAR), Sentinel-3 platform for multispectral imaging, radiometry and altimetry, Sentinel-4, Sentinel-5P and Sentinel-5 platforms for multispectral imaging and profiling, and Jason CS platform for operational altimetry for monitoring sea-surface height [9].

The Sentinel-2 performs multispectral imaging for land cover, land use, change detection maps; maps of biogeophysical variables such as leaf chlorophyll content, leaf water content, leaf area index; risk mapping; acquisition and rapid delivery of images to support disaster relief efforts [10]. The Sentinel-2 mission lifetime is 15 years. Its constellation comprises two identical satellites, Sentinel-2A launched 23 June 2015 and Sentinel-2B launched 7 March 2017. Satellites have sun-synchronous orbit at an altitude of 786 km (mean value) and together provide land coverage from −56° to +84° and global revisit time less than 5 days [11].

The MSI onboard Sentinel-2 satellites senses Earth surface in 13 spectral bands with spatial resolution of 10, 20, and 60 m. The main MSI band characteristics are given in Table 1.

Table 1. Spectral bands of the MSI sensor [11].

Band	Description	Central wavelength (nm)	Bandwidth (nm)	Spatial resolution, m
1	Coastal aerosol	443	20	60
2	Blue	490	65	10
3	Green	560	35	10
4	Red	665	30	10
5	Vegetation Red Edge	705	15	20
6	Vegetation Red Edge	740	15	20
7	Vegetation Red Edge	783	20	20
8	NIR	842	115	10
8A	Vegetation Red Edge	865	20	20
9	Water vapour	945	20	60
10	SWIR - Cirrus	1380	30	60
11	SWIR	1610	90	20
12	SWIR	2190	180	20

All data acquired by the MSI instrument are systematically processed to Level-1C that is released at no charge to users via the Copernicus Open Access Hub [12] and the US Geological Survey (USGS). The processing from Level-0 (decompressed raw data) to Level-1C involves radiometric correction, geometric viewing model refinement, data filtering, sharpening and resampling, conversion from radiances to reflectances, and data compression [13, 14]. Let us analyze possible influences of these processing stages on sensor noise model. After inversion of on-board equalization, data represent digital numbers measured by the sensor. At this level noise variance model for multi- and hyperspectral sensors utilizing photon counting detectors obey signal dependent model: $\sigma_n^2 = \sigma_0^2 + kI$, where σ_0^2 is variance of additive signal-independent component caused primary by sensor thermal noise, and kI is signal-dependent component caused by statistical nature of photon counting process [2]. Here k is a proportionality coefficient that we will call signal-dependency coefficients.

Stages of interest to this study, which modify sensor noise, are dark signal correction, deconvolution, denoising, conversion from radiances to reflectances, interpolation and compression.

Dark signal correction shifts all intensities by a fixed value: $I' = I + \Delta I$. Conversion from radiances to reflectances scales all intensities as: $I'' = vI$. These two linear transforms modify image intensity as $I''' = v(I + \Delta I)$. Noise variance model after these transformations becomes $\left(\sigma_n'''\right)^2 = v^2\left(\sigma_0^2 + k\left(\frac{I'''}{v} - \Delta I\right)\right) = \sigma_0^2 v^2 - \frac{k\Delta I}{v} + kvI'''$. It is seen that model type remains the same, only coefficients change.

Deconvolution and interpolation (e.g. bilinear interpolation) stages can be modeled as linear data filtering with a fixed data-independent kernel. Effect of such a filtering on noise model consists in noise variance decrease by a constant factor: $\sigma_n^2 \to \mu\sigma_n^2$, where μ equals squared sum of the kernel coefficients, and change in appearance of noise spatial correlation [15]. We model noise spatial correlation by Gaussian function $R_n(x_1, y_1, x_2, y_2) = R_n(x_1 - x_2, y_1 - y_2) = \sigma_n^2 \exp\left(-\frac{d^2}{2\sigma_{\text{Corr}}^2}\right)$, where $d = \sqrt{(x_2 - x_1)^2 + (y_2 - y_1)^2}$, (x, y) are spatial coordinates σ_{Corr}^2 is the parameter that determines unknown noise spatial correlation width (σ_{Corr} is distance in pixels where noise correlation drops to 0.6).

In contrast to previous stages, denoising and compression modify noise in a data-dependent way, thus changing noise model type. The filtering of MSI data and compression to JPEG2000 format are both based on wavelet shrinkage. Their primary effect on noise parameters are noise variance decrease and increase of noise spatial correlation width [15]. The magnitude of these effects is data-dependent and is determined by the true image structure (textural, homogeneous, heterogeneous with edges or small-sized objects), image texture characteristics (roughness) and noise level (signal-to-noise ratio, SNR) [6]. In this work, we restrict ourselves by the SNR influence on processed noise variance leaving more complex dependencies for a future study.

We model filtering and compression influence by introducing noise variance modification term in the form: $\sigma_{\text{np}}^2 = \sigma_{\text{n}}^2 \cdot g(SNR)$. The form of $g(SNR)$ should take into account that filtering/compression influence is negligible for large SNR values and increase monotonically with SNR decrease. In mathematical terms, we require $g(SNR_1) > g(SNR_2)$ for $SNR_1 > SNR_2$, $0 \le g(SNR) \le 1$, $\lim_{SNR \to \infty} g(SNR) = 1$. We analyze five two-parametric functions satisfying just above-mentioned conditions:

$$g(SNR, r, \alpha) = 1 - \frac{\alpha}{\left(r + SNR^{p_1}\right)^{p_2}},\ p_1 = 1,2,\ p_2 = 0.5,1, \text{ subject to } 0 \le \alpha \le r^{p_2},\ r \ge 0 \quad (1)$$

and

$$g(SNR, r, \alpha) = 1 - \alpha \cdot e^{-\frac{SNR}{r}}, \text{ subject to } 0 \le \alpha \le 1,\ r \ge 0. \quad (2)$$

For all $g(SNR)$ variants, we consider filtering/compression effect to be negligible for $SNR = 50$ and require

$g(50) > 0.99$. The full noise variance model

$$\sigma^2_{\text{np}}(I, SNR) = \left(\sigma_0^2 + kI\right) \cdot g\left(SNR, r, \alpha\right) \tag{3}$$

is bivariate and four-parametric. The filtering and compression stages should also modify noise spatial correlation width, but we consider this effect to be outside the scope of this paper. In our experiments we assumed noise spatial correlation width to be a constant yet unknown value for each band. For convince, in what follows we refer to noise influenced by SNR-dependent filtering and compression stages as processed noise, and noise with SNR-independent variance modeled by $\sigma_n^2 = \sigma_0^2 + kI$ as high-SNR noise. The high-SNR noise can be viewed as limit of processed noise for very high SNR values where filtering and compression effects are negligible. Note, that high-SNR noise is still processed due to interpolation and sharpening stages.

2.2 Parameters estimation of Sentinel-2 processed sensor noise

With the processing line of Sentinel-2 Level-1C data including filtering and compression stages, the sensor noise in the data becomes processed. In the paper, we leverage blind noise estimation approach to estimate parameters of noise variance model (3) for all MSI bands.

Blind noise parameter estimation has seen fast development in the last decade and now provides a set of methods applicable to a variety of scenarios [16] including multispectral (or color) [17] and hyperspectral images [2, 7, 18, 19]; signal-independent (additive) [20], Poisson [21] noise, or their mixture in the form of general model with signal-dependent noise variance [17, 19, 22-24]; methods with ability to characterize only noise variance [2, 17-23, 25] as well as noise spatial correlation properties [8, 24, 26]. Accuracy of these methods is high enough to consider them as an alternative to direct sensor calibration [2, 17, 18, 21, 23].

Estimating parameters of processed noise has been considered recently by Rakhshanfar and Amer in [15]. Their model of processed noise has similarity and dissimilarity to ours. In our work, similar to [15] we consider mixed Poissonian-Gaussian (signal-dependent) noise model and treat processed noise as non-white or spatially correlated. The method in [15] is more advantageous in that it considers arbitrary noise signal-dependency, more complex than $\sigma_n^2 = \sigma_0^2 + kI$. The proposed mvcNI+fBm is also capable to deal with arbitrary signal-dependency, but this is unnecessary for Sentinel-2 sensor and was not included in this paper. The method of Rakhshanfar and Amer processes color images in a channel-wise manner, while mvcNI+fBm is a vector method. The main difference is that we consider the bivariate model of processed noise variance, while the method in [15] is limited to an univariate model.

Existing methods for blind estimation of sensor noise parameters cannot be applied to the particular case of Sentinel-2 data because of the following reasons. The main reason is that no method can deal with multivariate noise variance model. In addition, methods for multi- and hyperspectral data require that all bands have the same spatial resolution and are spatially aligned, i.e. form 3D data or hypercube [7]. This is not the case for Sentinel-2 MSI data as bands have different spatial resolution (10, 20, 60m) with non-negligible inter-band misregistration.

We overcome all these drawbacks by (1) preprocessing Sentinel-2 MSI data and (2) modifying vcNI+fBm estimator earlier proposed by the authors to deal with multivariate noise variance model.

To properly form vector data we select a reference and several working MSI bands. In the vector data preparation, we would like to keep the reference band unmodified to have access to original Sentinel-2 Level-1C noise parameters. Each working band is aligned with the reference one to compensate for residual misregistration and interpolated to the reference band grid. To align working and reference bands, inter-band translation is estimated in 100 by 100 fragments. To match point spread function (PSF) of the reference and working bands, we select working bands with the same spatial resolution as that for the reference band, or higher. Working bands with higher spatial resolution are smoothed by averaging filter with kernel support δ_r by δ_r pixels, where δ_r is ratio of spatial resolutions of a pair of working and reference bands, then downsampled to the reference band resolution. For the tested MSI granules we found that inter-band translations between MSI bands are random values with standard deviation (SD) of about 0.5-0.8 pixels.

Selected combinations of reference and working bands are listed in Table 2. We found three working bands to be sufficient for estimating Sentinel-2 noise parameters. In cases when more than three bands can be used as working bands, those with nearest wavelengths were selected to ease reference-working bands spectral decorrelation.

The vcNI+fBm is naturally suitable for the problem of parameter estimation of multivariate noise model. It was originally proposed in [2] for spatially uncorrelated noise and extended to correlated noise in [8]. The vcNI+fBm consists of two parts, one responsible for estimating noise parameters locally from small image patches (estimation stage), another for aggregating local estimates into global noise model (fitting stage). Spatial locality of the estimation stage allows abstracting from a particular noise model. It can be assumed that model parameters do not vary significantly within local image patch and estimated parameters correspond to a particular point in (I, SNR) space. The fitting stage abstracts from the image data and works with noise parameter estimates to obtain noise variance model parameter vector $(\sigma_0^2, k, r, \alpha)$. The version of vcNI+fBm that is able to deal with multivariate noise model will be later referred to as mvcNI+fBm.

Table 2. Reference and working bands for estimating Sentinel-2 noise parameters.

Reference band	Working bands	Reference band	Working bands
1	2, 3, 4	8	2, 3, 4
2	3, 4, 8	8A	6, 7, 8
3	2, 4, 8	9	7, 8, 8A
4	2, 3, 8	10	8A, 9, 11
5	4, 6, 7	11	8, 8A, 12
6	4, 5, 7	12	8, 8A, 11
7	5, 6, 8	-//-	-//-

For each reference band, the preprocessed MSI data are fed into the mvcNI+fBm estimator of noise parameters. The estimation stage of mvcNI+fBm is a local maximum likelihood estimator of sensor band noise variances, noise spatial correlation width, image texture amplitude, inter-band correlation of image texture, and texture roughness under parametrical 2D fractal Brownian motion (fBm) model for the image texture and Gaussian distribution of noise. The general scheme on Sentinel-2 noise parameter estimation by mvcNI+fBm is shown in Fig. 1.

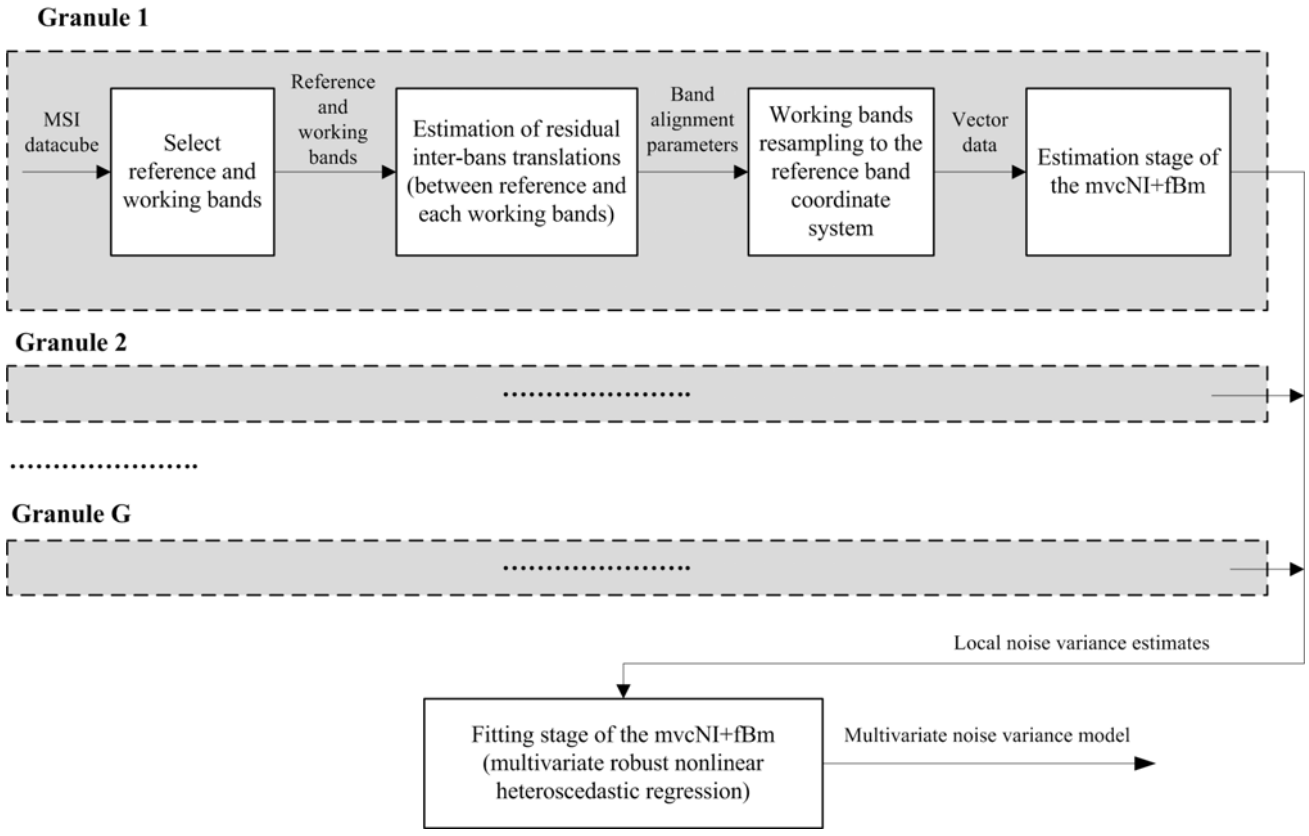

Figure. 1. Generalized scheme of estimation of noise parameters of Sentinel-2 sensor by the mvcNI+fBm.

The output of estimation stage mvcNI+fBm is a set of noise band variance estimates $\hat{\boldsymbol{\sigma}}^2_{n.i} = \left(\hat{\sigma}^2_{n.1i}, \hat{\sigma}^2_{n.2i}, ..., \hat{\sigma}^2_{n.mi}\right)$ and correlation width $\sigma_{corr.i}$ for local fragments with mean intensity $\mathbf{I}_i = \left(I_{1i}, I_{2i}, ..., I_{mi}\right)$ and local SNR $\mathbf{SNR}_i = \left(SNR_{1i}, SNR_{2i}, ..., SNR_{mi}\right)$, where $i = 1...N_{\text{fr}}$, N_{fr} is number of fragments, m is number of bands. Local SNR for i-th fragment of j-th band is estimated as $\widehat{SNR}_{ji} = \sqrt{\left(V_{ji} - \hat{\sigma}^2_{n.ji}\right) / \hat{\sigma}^2_{n.ji}}$ for $V_{ji} > \hat{\sigma}^2_{n.ji}$ and $\widehat{SNR}_{ji} = 0$ for $V_{ji} \le \hat{\sigma}^2_{n.ji}$, where V_{ji} is variance of the fragment intensity. For all variance estimates their estimation SDs (derived from the Fisher Information Matrix, FIM) are also provided: $\hat{\boldsymbol{\sigma}}_{\text{var}.i} = \left(\hat{\sigma}_{\text{var}.1i}, \hat{\sigma}_{\text{var}.2i}, ..., \hat{\sigma}_{\text{var}.mi}\right)$. The estimation stage is common to vcNI+fBm and mvcNI+fBm.

Noise variance estimates can be used to evaluate sensor noise model in linear or nonlinear form. Notice, that each measurement is characterized by its own accuracy, therefore regression problem becomes heteroscedastic. For the mixture of additive and scaled Poisson noises, regression problem is univariate and linear: $\sigma^2_{n.1}\left(I\right) = \sigma^2_0 + kI_1$. Regression coefficients are found by solving optimization problem:

$$\left(\hat{\sigma}^2_0, \hat{k}\right) = \arg\min_{\sigma_0, k}\left(\sum_{i=1}^{N_{\text{fr}}} \frac{\left(\sigma^2_0 + kI_{1i} - \hat{\sigma}^2_{n.1i}\right)^2}{\hat{\sigma}^2_{\text{var}.1i}}\right). \tag{4}$$

Here we estimate noise model parameters only for the reference band (with index 1). The rest of estimates for working bands are not used, as they are modified by image preprocessing procedure. The particular fitting stage (4) was considered in the vcNI+fBm estimator.

In case of processed noise, SNR variable is added to the noise variance model, and regression problem becomes bivariate and nonlinear: $\sigma^2_{n.1}\left(I_1, SNR_1\right) = \left(\sigma^2_0 + kI_1\right) \cdot g\left(SNR_1, r, \alpha\right)$. Regression coefficients are found by solving optimization problem:

$$\left(\hat{\sigma}^2_0, \hat{k}, \hat{r}, \hat{\alpha}\right) = \arg\min_{\sigma_0, k, r, \alpha}\left(\sum_{i=1}^{N_{\text{fr}}} \frac{\left(\left[\sigma^2_0 + kI_{1i}\right] \cdot g\left(SNR_{1i}, \alpha, r\right) - \hat{\sigma}^2_{n.1i}\right)^2}{\hat{\sigma}^2_{\text{var}.1i}}\right). \tag{5}$$

The advantage of the mvcNI+fBm approach is that by selecting only Noise Informative fragments (fragments providing noise variance estimates with a predefined accuracy), it significantly reduces the number of outliers. Nevertheless, the presence of outliers cannot be neglected. We adopted the simplest robust regression approach [27] using the so-called 'talwar' weighting function [28]: $w(r) = \left(abs(r) < 1\right)$, where r defines scaled residuals. In calculating scaled residuals, we use standard deviation (SD) of each noise parameter estimate evaluated by the mvcNI+fBm to take into account regression problem heteroscedasticity and we define $r = \dfrac{\hat{\sigma}^2_n - \hat{\sigma}^2_{n.\text{pr}}}{\hat{\sigma}_{\text{var}}} \dfrac{1}{T\sigma_{\text{norm}}\sqrt{1-h}}$, where $\hat{\sigma}^2_{n.\text{pr}}$ is the prediction of a parameter σ^2_n at the current iteration of robust regression by model (3), $\hat{\sigma}^2_n - \hat{\sigma}^2_{n.\text{pr}}$ are heteroscedastic residuals, $(\hat{\sigma}^2_n - \hat{\sigma}^2_{n.\text{pr}}) / \hat{\sigma}_{\text{var}}$ are normalized homoscedastic residuals, T is the tuning constant, σ_{norm} is an estimate of the SD of the normalized residuals (related to the statistical efficiency of the mvcNI+fBm estimator as $e = 1/\sigma^2_{\text{norm}}$), h is leverage. For the mvcNI+fBm algorithm, the value of T is experimentally set as 4; σ_{norm} is evaluated as MAD (Median Absolute Deviation) of normalized residuals multiplied by 1.48 for providing estimation robustness [29].

To characterize the prediction quality of regression models, we used generalized determination coefficient [30]: $R^2 = 1 - \exp\left(-\dfrac{2}{N_{\text{fr}}}\left(l_R - l_U\right)\right)$, where l_R is the log-likelihood for regression model restricted only with intercept, l_u is the log-likelihood of the unrestricted regression model. Assuming normal distribution of noise parameter estimate errors provided by the mvcNI+fBm and omitting constants shared by both l_R and l_u, the log-likelihoods for restricted and

unrestricted models take the following quite simple form: $l_R = -\frac{1}{2}\sum_{i=1}^{N_{fr}} \frac{\left(\hat{\sigma}^2_{n.i} - \hat{\sigma}^2_{n.\text{const}}\right)^2}{\hat{\sigma}^2_{\text{var.i}}}$ and $l_u = -\frac{1}{2}\sum_{i=1}^{N_{fr}} \frac{\left(\hat{\sigma}^2_{n.i} - \hat{\sigma}^2_{n.\text{pr.i}}\right)^2}{\hat{\sigma}^2_{\text{var.i}}}$.

3. SENTINEL-2 MSI SENSOR NOISE PARAMETERS ESTIMATION FROM REAL DATA

3.1 Test data description

Our Sentinel-2 MSI sensor noise analysis is based on six granules described in Table 3. All tiles were downloaded through the USGS EarthExplorer service. In selecting tiles for analysis, the goal was to cover for each tile as wide intensity range as possible. Therefore, all tiles represent water (typically the darkest image object), land (intermediate intensity range) and clouds (the brightest object on an image). Presence of water and land is assured by selecting tiles covering seashore, lake shores, rivers, bays etc. We searched among tiles with cloud cover ranging from 20 to 50%. An example of analysis tile is shown in Fig. 2.

Table 3. Description of Sentilel-2A granules selected for estimating MSI noise parameters.

Granule index	Entity ID	Acquisition Date	Center coordinates (Lon, Lat)	Cloud cover, %
1	S2A_OPER_MSI_L1C_TL_SGS__20160721T084726_20160721T123307_A005638_T36UYA_N02_04_01	2016/07/21	50.0040061, 36.5568571	45.5069
2	S2A_OPER_MSI_L1C_TL_SGS__20161113T112905_20161113T145909_A007284_T30UWV_N02_04_01	2016/11/13	49.1564453, -2.2473208	26.2669
3	L1C_T33SWC_A007941_20161229T095556	2016/12/29	38.3525590, 15.6280919	35.0718
4	S2A_OPER_MSI_L1C_TL_SGS__20161106T113523_20161106T150452_A007184_T30UVV_N02_04_01	2016/11/06	49.1572387, -3.6191042	43.9848
5	L1C_T35TNF_A008441_20170202T090155	2017/02/02	41.0554680, 27.6530904	30.0324
6	S2A_OPER_MSI_L1C_TL_SGS__20160825T044116_20160825T095100_A006136_T47VPC_N02_04_01	2016/08/25	56.3252616, 101.5050369	20.3338

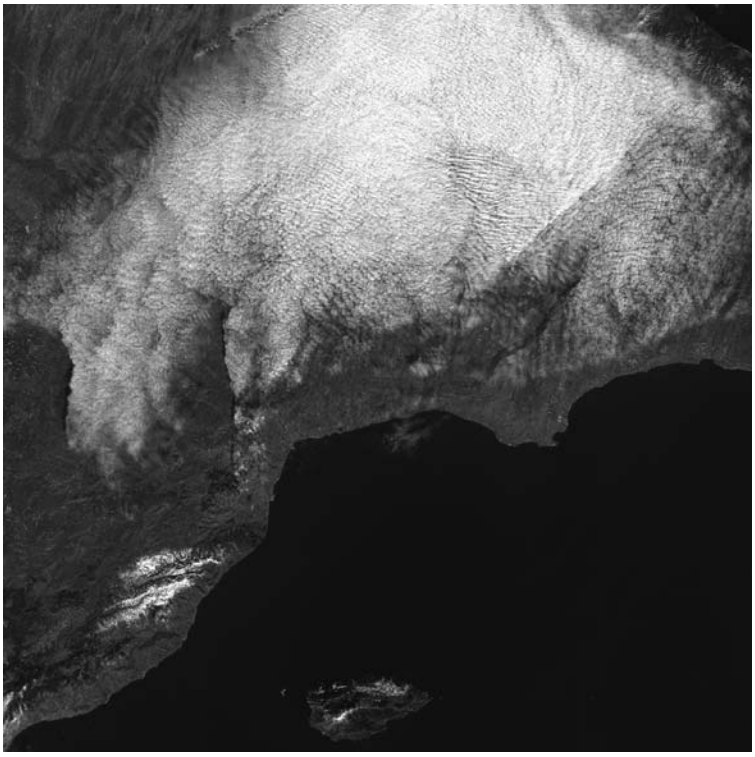

Figure. 2. Band #4 of granule 5. Intensity range is from 0 (black) to 6000 (white).

3.2 Noise variance estimates analysis for a single band

Let us first analyze Sentinel-2 results obtained with the mvcNI+fBm for band #4. The noise variance estimates in the (Intensity, Variance) plane are shown in Fig. 3 for each considered granule. For each granule the univariate noise model $\sigma_n^2 = \sigma_0^2 + kI$ is shown as a straight line. The univariate model is calculated according to (4) using data collected from all granules and patches with SNR greater than 15 to avoid processed noise influence. The estimates reveal that noise variance linearly increases with intensity as signal-dependency model suggests; estimates are consistent for all granules; estimates concentrate around fitted line but have significant number of outliers. Low SNR estimates can be seen to cluster below the fitted univariale model (e.g. for granule #2 and #4); this effect is due to filtering/compression influence. Following these observations, for each band, we aggregate together variance estimates for all granules to perform nonlinear regression (5).

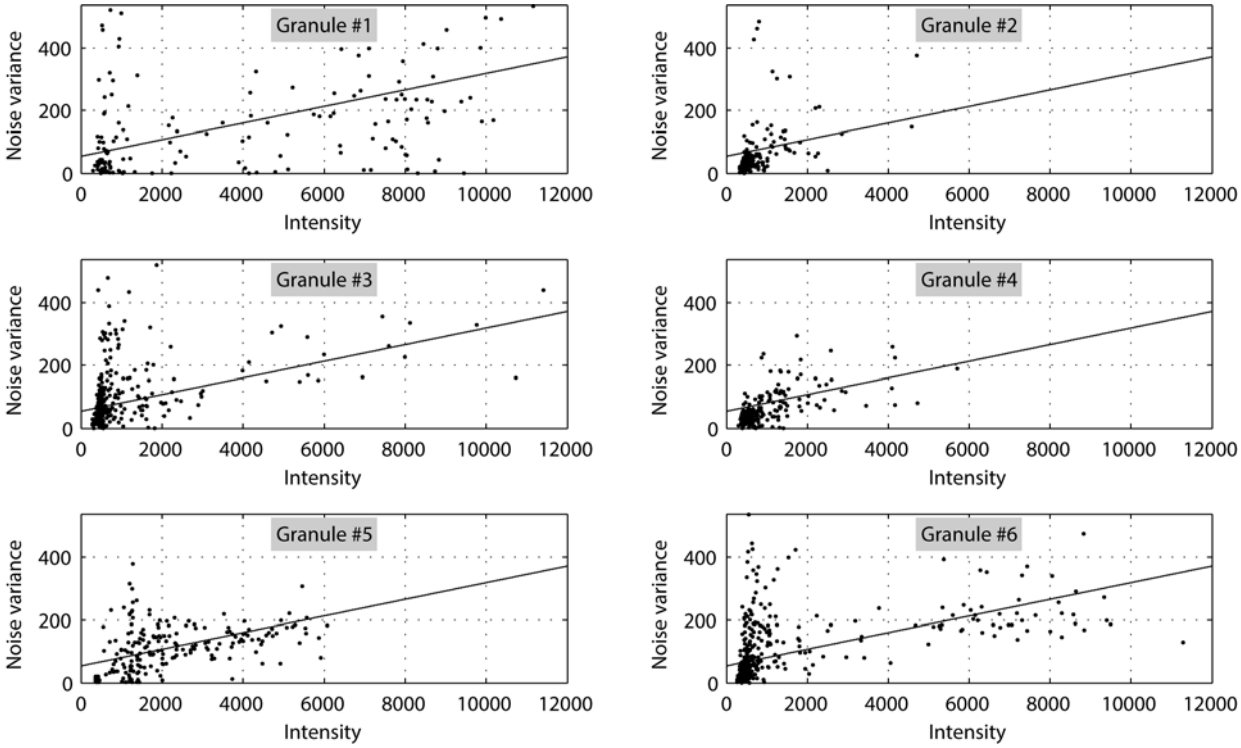

Figure 3. Noise variance estimates obtained by the mvcNI+fBm for band #4. Fitted univariate model $\sigma_n^2 = \sigma_0^2 + kI$ is shown as straight black line.

Dependence of σ_{np}^2 on SNR can be visualized by normalizing σ_{np}^2 on fitted univariate model $\hat{\sigma}_0^2 + \hat{k}I$: $\hat{\sigma}_{np.norm.i}^2 = \hat{\sigma}_{np.i}^2 / (\hat{\sigma}_0^2 + \hat{k}I_i)$. Normalized estimates are shown in Fig. 4 as a function of SNR. To better reveal dependence on SNR, noise variance estimates were aggregated in intervals 0…0.25, 0.25…0.5, 0.5…0.75, … according to their SNR value. Median value of noise variance in each interval is shown in Fig. 4. The decrease of noise variance with SNR decrease can be seen well.

Estimates of noise variance model parameters for the considered model variants (one univariate and five bivariate) are shown in Table 4 and in Fig. 4 in graphical form. For each model variant, coefficient of determination (R squared, expressed in %), model parameter estimates, estimation SD, and t-statistic [31] are given. It is seen that R squared for bivariate models (more than 99%) is significantly higher than that for univariate model (about 65%). Therefore, SNR influence on noise variance is significant. All bivariate models yield almost identical results. This is well seen from Fig. 4. We selected the model 2 for future study as it has physically interpretable parameters: the value $1-\alpha$ is ratio of noise variance at zero SNR and variance high-SNR noise (for SNR approaching infinity). For example, for band #4 $\alpha = 0.7841$, $1-\alpha \approx 0.21$. This means that for very homogeneous areas noise variance is reduced by a factor of 5 as compared to high-SNR noise.

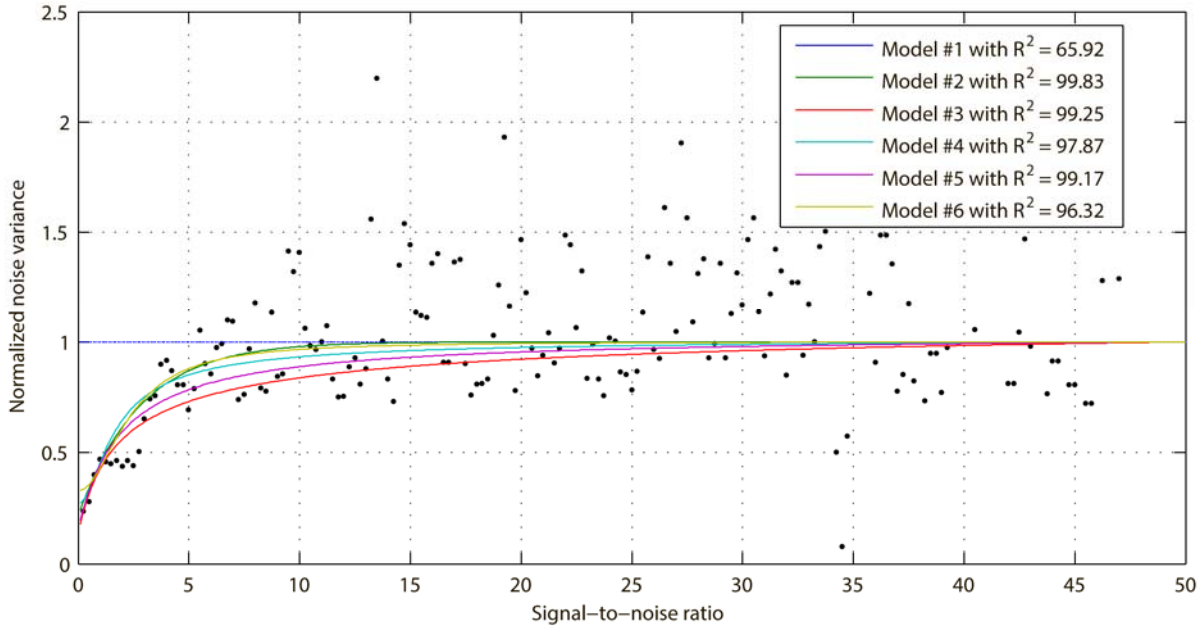

Fig. 4. Normalized noise variance estimates vs. SNR for band #4.

Table 4. Estimates of bivariate sensor noise model parameters for band #4 of Sentinel-2 MSI sensor.

Model index	Model type	$R^2 \cdot 100\%$	Parameters	Parameter SDs	t-stats
1	$\sigma_{np}^2 = \sigma_0^2 + kI$	65.92	$\sigma_0^2 = 54.07;\ k = 0.0265$	3.2358; 0.0013	16.71; 20.04
2	$\sigma_{np}^2 = \left(\sigma_0^2 + kI\right)\left(1 - \alpha \cdot e^{-\frac{SNR}{r}}\right)$	99.83	$\sigma_0^2 = 53.32;\ k = 0.0272;$ $r = 2.7893;\ \alpha = 0.7841$	1.8529; 0.0009; 0.2098; 0.0118	28.78; 31.76; 13.29; 66.43
3	$\sigma_{np}^2 = \left(\sigma_0^2 + kI\right)\left[1 - \frac{\alpha}{\sqrt{r + SNR}}\right]$	99.25	$\sigma_0^2 = 62.0582;\ k = 0.0287;$ $r = 0.9884;\ \alpha = 0.8797$	2.1797; 0.0009; 0.1190; 0.0485	28.47; 32.43; 8.31; 18.13
4	$\sigma_{np}^2 = \left(\sigma_0^2 + kI\right)\left[1 - \frac{\alpha}{\sqrt{r + SNR^2}}\right]$	97.87	$\sigma_0^2 = 52.7240;\ k = 0.0285;$ $r = 1.3087;\ \alpha = 0.8376$	1.7101; 0.0009; 0.1798; 0.0560	30.83;33.40 7.28; 14.95
5	$\sigma_{np}^2 = \left(\sigma_0^2 + kI\right)\left[1 - \frac{\alpha}{(r + SNR)}\right]$	99.17	$\sigma_0^2 = 57.5606;\ k = 0.0282;$ $r = 1.9805;\ \alpha = 1.6875$	2.0570; 0.0009; 0.1979; 0.1602	27.98; 32.71; 10.01; 10.53
6	$\sigma_{np}^2 = \left(\sigma_0^2 + kI\right)\left[1 - \frac{\alpha}{\left(r + SNR^2\right)}\right]$	96.32	$\sigma_0^2 = 53.2888;\ k = 0.0275;$ $r = 5.5835;\ \alpha = 3.7418$	1.7614; 0.0009; 0.7246; 0.4836	30.25; 32.13; 7.70; 7.74

3.3 Sentinel-2 noise variance parameters band-to-band variation

Estimates of bivariate noise variance model parameters obtained with the mvcNI+fBm are presented in Table 5 and in Figures 5 and 6. Parameter estimates are reliable (with t-stats greater than 4) for all bands except for bands ##1, 10. For this band, experiments with a larger amount of image data are necessary. For bands with reliable estimates, signal-independent noise variance varies from 26 to 103; signal-dependency coefficient varies from 0.011 to 0.0523. Noise variance dependence on SNR is similar for bands ##2, 4, 5, 6, 7, 8, 8A, 11. For these bands, the MSI sensor noise is not influenced by filtering/compression for SNR exceeding 15. The ratio between variance of high-SNR noise and noise in homogeneous areas varies from 2 to 5 with mean value about 2.5. These values indicate that statistics of processed and high-SNR noise differ significantly for MSI sensor of Sentinel-2A satellite and this difference should be taken into account in designing processing algorithms of MSI data. For bands ##3 and 9, a different noise variance dependence on SNR could be attributed both to specific Level-1C data processing chain and by lack of the data used to collect mvcNI+fBm estimates. Experiments with a larger amount of image data are also needed for these bands. For all bands

noise correlation width estimates (σ_{corr}) obtained with the mvcNI+fBm have mean value about 0.45 pixels. This spatial correlation of noise is caused by the influence of a mixture factors including interpolation, filtering and compression.

Table 5. Estimates of bivariate noise variance model (model #2) parameters for all MSI bands.

Band	$R^2 \cdot 100\%$	Parameters							
		σ_0^2		k		r		α	
		estimate	t-stats	estimate	t-stats	estimate	t-stats	estimate	t-stats
1	96.8	217.98	3.62	0.0416	2.54	55.2136	1.33	0.9896	148.67
2	79.5	75.74	15.08	0.0238	17.93	7.5157	7.95	0.6564	41.22
3	81.2	26.35	36.79	0.0149	38.79	0.7587	7.55	0.6820	15.83
4	99.8	53.32	28.78	0.0272	31.76	1.3087	13.29	0.7841	66.43
5	89.8	27.49	15.65	0.0126	13.47	5.4099	4.08	0.5204	16.26
6	98.2	42.92	16.17	0.0186	15.49	4.9360	4.96	0.6403	24.94
7	96.8	71.66	11.31	0.0296	10.02	4.1682	4.65	0.7786	28.62
8	98.9	92.82	22.96	0.0283	29.53	7.0336	12.66	0.8132	96.80
8A	99.5	103.11	16.00	0.0345	13.15	4.6334	6.66	0.8013	44.97
9	98.9	38.19	12.89	0.0523	10.83	19.6955	5.79	0.8989	87.02
10	79.6	9.84	1.66	0.0103	1.65	16.1909	1.14	0.8994	12.76
11	99.7	31.65	61.63	0.0114	29.01	3.3978	24.28	0.8033	82.73
12	99.2	54.65	22.22	0.0223	17.35	18.3261	8.70	0.8114	78.62

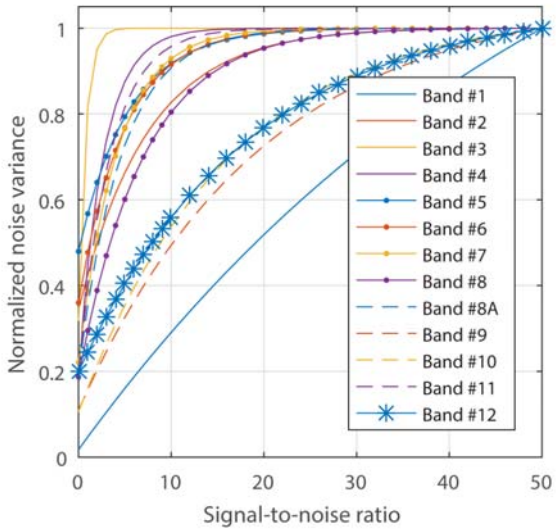

Fig. 5. Noise variance dependence on SNR for all bands of MSI sensor

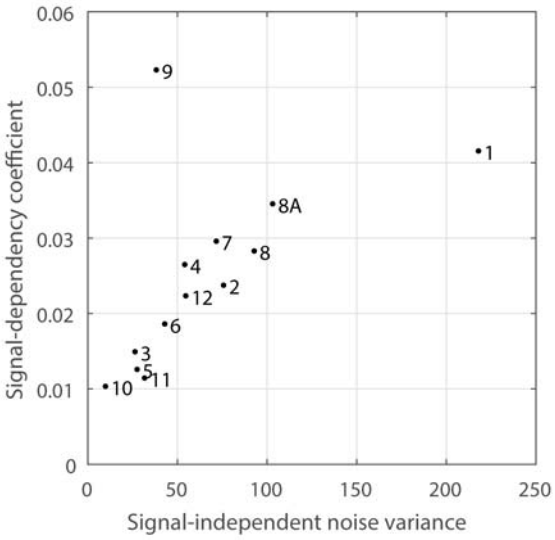

Fig. 6. Signal-independent component variance and signal-dependency coefficient for all bands of MSI sensor

4. CONCLUSIONS

This paper deals with the problem of estimating noise variance model of Sentinel-2 MSI sensor at the Level-1C data. The absence of noise model parameters in Sentinel-2 metadata as well as calibration data suggest using blind noise parameter estimation approach that extracts information of sensor noise directly from noisy images. We demonstrate that filtering and compression procedures applied during preparation of Level-1C Sentinel-2 data modifies noise variance model. In addition to dependency on image intensity it becomes dependent on local SNR value. Therefore, processed noise variance model is bivariate. Existing blind noise parameter estimation approaches are restricted to univariate noise model (with signal-dependent component being function of image intensity) and cannot be applied to Level-1C Sentinel-

2 data.

We have proposed an extension of existing vcNI+fBm method to multivariate data, mvcNI+fBm estimator. It comprises two stages: estimation stage is responsible for extracting noise variance estimates from local image patches where image intensity and SNR can be treated as constant, fitting stage fits nonlinear multivariate regression model to raw noise variance estimates.

Using six Sentinel-2A granules, we have demonstrated that dependence of Level-1C noise variance on SNR is significant for all bands: taking this parameter into account increases R squared of regression model to 94% in average as compared to 42% for univariate signal-dependent model. According to our estimates, filtering/compression influence is negligible for SNR exceeding 15. Noise variance monotonically decreases with SNR decrease below 15. Noise variance reduction is about 2 - 5 times for homogeneous areas as compared to variance of high-SNR noise.

The flexibility of the proposed method allows considering complex noise models. Interesting direction of future research is including image texture roughness as an additional parameter influencing noise variance change after filtering/compression procedures.

REFERENCES

[1] F. Spoto, O. Sy, P. Laberinti *et al.*, "Overview Of Sentinel-2," 2012 IEEE International Geoscience and Remote Sensing Symposium. 1707-1710 (2012).

[2] M. L. Uss, B. Vozel, V. V. Lukin *et al.*, "Local Signal-Dependent Noise Variance Estimation From Hyperspectral Textural Images," IEEE J. Sel. Topics Signal Process., 5(3), 469-486 (2011).

[3] A. N. Zemliachenko, R. A. Kozhemiakin, M. L. Uss *et al.*, "Lossy compression of hyperspectral images based on noise parameters estimation and variance stabilizing transform," Journal of Applied Remote Sensing, 8(1), 083571-083571 (2014).

[4] V. V. Lukin, S. S. Krivenko, M. S. Zriakhov *et al.*, "Lossy compression of images corrupted by mixed Poisson and additive Gaussian noise," 2009 International Workshop on Local and Non-Local Approximation in Image Processing. 33-40 (2009).

[5] P. Chatterjee, and P. Milanfar, "Practical Bounds on Image Denoising: From Estimation to Information," Image Processing, IEEE Transactions on, 20(5), 1221-1233 (2011).

[6] M. Uss, A. Rubel, V. Lukin *et al.*, "Lower bound on image filtering mean squared error in the presence of spatially correlated noise," Microwaves, Radar and Remote Sensing Symposium (MRRS), 2014 IEEE. 10-13 (2014).

[7] G. Lianru, D. Qian, Z. Bing *et al.*, "A Comparative Study on Linear Regression-Based Noise Estimation for Hyperspectral Imagery," IEEE J. Sel. Topics Appl. Earth Observ. in Remote Sens., 6(2), 488-498 (2013).

[8] M. L. Uss, B. Vozel, V. V. Lukin *et al.*, "Maximum likelihood estimation of spatially correlated signal-dependent noise in hyperspectral images," Optical Engineering, 51(11), 111712-1-111712-11 (2012).

[9] Y. L. Desnos, M. Borgeaud, M. Doherty *et al.*, "The European Space Agency's Earth Observation Program," IEEE Geoscience and Remote Sensing Magazine, 2(2), 37-46 (2014).

[10] Scentinel program overview, Europenian Space Agency. Available: http://www.esa.int/Our_Activities/Observing_the_Earth/Copernicus/Overview4

[11] M. Drusch, U. Del Bello, S. Carlier *et al.*, "Sentinel-2: ESA's Optical High-Resolution Mission for GMES Operational Services," Remote Sensing of Environment, 120, 25-36 (2012).

[12] Copernicus Open Access Hub. Available: https://scihub.copernicus.eu/

[13] Scentinel-2 MSI Technical Guide. Available: https://earth.esa.int/web/sentinel/technical-guides/sentinel-2-msi/products-algorithms

[14] [Sentinel-2 User Handbook] European Space Agency (ESA) (2015).

[15] M. Rakhshanfar, and M. A. Amer, "Estimation of Gaussian, Poissonian–Gaussian, and Processed Visual Noise and Its Level Function," IEEE Transactions on Image Processing, 25(9), 4172-4185 (2016).

[16] B. Vozel, S. Abramov, K. Chehdi *et al.*, [Blind determination of noise type for spaceborne and airborne remote sensing] Wiley-ISTE, 9 (2010).

[17] C. Liu, R. Szeliski, S. B. Kang *et al.*, "Automatic Estimation and Removal of Noise from a Single Image," Pattern Analysis and Machine Intelligence, IEEE Transactions on, 30(2), 299-314 (2008).

[18] L. Alparone, M. Selva, B. Aiazzi *et al.*, "Signal-dependent noise modelling and estimation of new-generation imaging spectrometers," Hyperspectral Image and Signal Processing: Evolution in Remote Sensing, 2009. WHISPERS '09. First Workshop on. 1-4 (2009).
[19] N. Acito, M. Diani, and G. Corsini, "Signal-Dependent Noise Modeling and Model Parameter Estimation in Hyperspectral Images," IEEE Trans. Geosci. Remote Sens., 49(8), 2957-2971 (2011).
[20] D. Zoran, and Y. Weiss, "Scale invariance and noise in natural images," Computer Vision, 2009 IEEE 12th International Conference on. 2209-2216 (2009).
[21] A. Foi, M. Trimeche, V. Katkovnik *et al.*, "Practical Poissonian-Gaussian Noise Modeling and Fitting for Single-Image Raw-Data," Image Processing, IEEE Transactions on, 17(10), 1737-1754 (2008).
[22] L. Azzari, and A. Foi, "Gaussian-Cauchy mixture modeling for robust signal-dependent noise estimation," Acoustics, Speech and Signal Processing (ICASSP), 2014 IEEE International Conference on. 5357-5361 (2014).
[23] M. L. Uss, B. Vozel, V. V. Lukin *et al.*, "Image informative maps for component-wise estimating parameters of signal-dependent noise," J. Electron. Imaging, 22(1), 013019-013019 (2013).
[24] M. Colom, M. Lebrun, A. Buades *et al.*, "Nonparametric Multiscale Blind Estimation of Intensity-Frequency-Dependent Noise," Image Processing, IEEE Transactions on, 24(10), 3162-3175 (2015).
[25] B. Aiazzi, L. Alparone, S. Baronti *et al.*, "Unsupervised estimation of signal-dependent CCD camera noise," EURASIP Journal on Advances in Signal Processing, 2012(1), 1-11 (2012).
[26] N. N. Ponomarenko, V. V. Lukin, K. O. Egiazarian *et al.*, "A method for blind estimation of spatially correlated noise characteristics," SPIE 7532, Image Processing: Algorithms and Systems VIII. 7532, 753208-753208-12 (2010).
[27] R. Andersen, [Modern methods for robust regression] Sage University Paper Series on Quantitative Applications in the Social Sciences, (2008).
[28] M. J. Hinich, and P. P. Talwar, "A Simple Method for Robust Regression," Journal of the American Statistical Association, 70(349), 113-119 (1975).
[29] P. J. Huber, [Robust statistics] Springer Berlin Heidelberg, (2011).
[30] L. Magee, "R 2 Measures Based on Wald and Likelihood Ratio Joint Significance Tests," The American Statistician, 44(3), 250-253 (1990).
[31] G. A. Seber, and A. J. Lee, [Linear regression analysis] John Wiley & Sons, (2012).